Vol. 89: 85–98, 2023
https://doi.org/10.3354/cr01709

CLIMATE RESEARCH
Clim Res

Published online February 2

High-temperature indicators for capturing the impacts of heat stress on yield: lessons learned from irrigated wheat in the hot and dry environment of Sudan

Toshichika Iizumi[1,2,*], Mitsuru Tsubo[2], Atsushi Maruyama[1], Izzat S. A. Tahir[3], Yasunori Kurosaki[2], Hisashi Tsujimoto[2]

[1]Institute for Agro-Environmental Sciences, National Agriculture and Food Research Organization, Tsukuba, Ibaraki 305-8604, Japan

[2]Arid Land Research Center, Tottori University, Tottori 680-0001, Japan

[3]Gezira Research Station, Agricultural Research Corporation, P.O. Box 126, Wad Medani, Sudan

ABSTRACT: High temperatures occurring during flowering and early grain filling substantially decrease cereal yields. Drawing on accumulated evidence showing that, compared to air temperature (Ta), crop canopy temperature (Tc) better explains observed yield reductions caused by heat stress, we evaluated the usefulness of Tc versus Ta in designing high-temperature indicators for agrometeorological services, including crop monitoring and forecasting. The hot and dry environment of Sudan provides an ideal testbed. Tc was derived from the combined simulation of a crop model and a land surface model. Based on regressions linking the high-temperature indicators with irrigated wheat yield variations in 3 regions of Sudan over the last half-century, we found that using phenological periods rather than months for the wheat season (November to February), and using Tc rather than Ta, more effectively tracks the adverse effects of high temperature on yield during the key periods. The Tc-based indicators calculated for the key phenological periods have more robust multi-region applicability than the Ta-based indicators calculated for months and season, although they do not necessarily outperform the region-specific indicators in terms of explanatory power. We determined that the key periods were the vegetative growth period for the relatively cool region, and the reproductive growth period for the relatively hot regions. These findings suggest that agrometeorological services at the national and global levels should adopt Tc-based indicators, which will ultimately help players in global food systems adapt to climate change by preparing for wheat supply disruptions due to high-temperature extremes.

KEY WORDS: Canopy temperature · Heat stress · Sector-specific climate indices · Agrometeorological service

1. INTRODUCTION

Observed increases in the frequency, intensity, and duration of high-temperature extremes under climate change pose challenges for crop production, especially in the hot and dry regions of the world (Mbow et al. 2019). High temperatures (heat stress) occurring during flowering and early grain filling substantially decrease the yields and grain quality of cereals, including wheat (Asseng et al. 2015, 2017, 2019, Barlow et al. 2015, Rezaei et al. 2015a, Tack et al. 2015). Accumulated evidence indicates that crop canopy tem-

*Corresponding author: iizumit@affrc.go.jp

Publisher: Inter-Research · www.int-res.com

perature (Tc) better explains observed yield reductions caused by heat stress than does air temperature (Ta) (Siebert et al. 2014, Rezaei et al. 2015a). Consequently, efforts have continued to improve process-based crop models by using Tc to simulate the heat stress effect on grain number, accelerated leaf senescence, and yield (Jamieson et al. 1995, Brisson et al. 1998, Yoshimoto et al. 2011, van Oort et al. 2014, Webber et al. 2016, 2017). However, no attempt has been made to apply Tc to climate indices for agricultural monitoring and forecasting, although sector-specific climate indices have been discussed (for instance, by the Expert Team on Climate Information for Decision-Making of the World Meteorological Organization; WMO 2021).

As a first step, a statistical analysis comparing the explanatory power of Tc for yield relative to Ta offers useful insights. The difference between Tc and Ta for irrigated crops becomes substantial under dry atmospheric conditions with variations in air humidity, CO_2 concentration, and crop varietal characteristics (Amani et al. 1996, Fukuoka et al. 2012, Yoshimoto et al. 2012, Siebert et al. 2014, Shew et al. 2020). The hot and dry environment of Sudan, where the hottest wheat-producing conditions in the world occur, and where wheat is grown under fully irrigated conditions (Negassa et al. 2013, Martre et al. 2017), provides an ideal testbed to assess the potential of applying Tc to high-temperature indicators in agrometeorological services. The well-documented occurrence of wheat yield reductions under high-temperature conditions in Sudan (Asseng et al. 2017, Iizumi et al. 2021a) further underscores the validity of this case selection.

Musa et al. (2021) presented a correlation analysis between yield and 4 Ta-based high-temperature indicators for 3 regions in Sudan (Dongola, Wad Medani, and New Halfa) using data from 48 seasons (1970/71 to 2017/18). The indicators included average daily maximum and minimum air temperatures (Tmax and Tmin), total hot days (THD), and total hot nights (THN). Each indicator was calculated for individual months and for the entire wheat season (November, December, January, February: NDJF). Musa et al. (2021) found that the departures of yield from the trend line (yield anomalies) significantly negatively correlated with one of the indicators calculated for the season, with a Pearson correlation coefficient from −0.41 for THN in Dongola to −0.43 for Tmax in Wad Medani to −0.55 for Tmin in New Halfa. However, no single indicator explained the yield anomalies across the regions, posing a challenge in designing robust climate indices for which multi-region applicability is a prerequisite.

We sought to evaluate the usefulness of Tc relative to Ta in designing high-temperature indicators by addressing the following 3 questions: (1) Is using Tc as a predictor in a statistical model more powerful than using Ta to explain yield anomalies associated with heat stress? (2) Does the consideration of crop phenology in the high-temperature indicator calculation increase its explanatory power as compared to indicators calculated for calendar months and season? (3) Does a nonlinear specification outperform a linear specification in associating high-temperature indicators with yield anomalies? The aim of the second question was to distinguish between the effect on yield from the consideration of crop phenology alone and the effect from crop phenology plus Tc, which has implications for the use of a crop phenology model in agrometeorological services. The third question was included in order to test the relative benefits of considering nonlinear temperature effects on yield through the specification of statistical models for agrometeorological services for a large spatial domain (e.g. national to global scales), given that the temperature effects on yield reported in earlier studies are diverse, from relatively linear (Amani et al. 1996, Asseng et al. 2015, 2017, Iizumi et al. 2021a) to highly nonlinear (Lobell et al. 2012, Tack et al. 2015, Shew et al. 2020). The findings from this study are expected to add evidence from the hot and dry environments of Sudan of the benefits of using Tc to capture the adverse effects of heat stress on yield that have been previously reported.

2. METHODS

The methodological overview in this study is presented in Fig. 1. The sub-sections that follow describe the crop data (Section 2.1) and weather data (Section 2.2) used, as well as the calculation of Tc using a crop model and a land surface model (Section 2.3). The high-temperature indicators calculated from Ta and Tc are then described (Section 2.4). Finally, the regression analyses that associate the high-temperature indicators with yield anomalies are discussed (Section 2.5).

2.1. Crop data

Wheat production, cultivated and harvested areas, and yield in the 3 studied regions for the 50 seasons from 1970/71 to 2019/20 were obtained from the Federal Ministry of Agriculture and Forestry in Sudan.

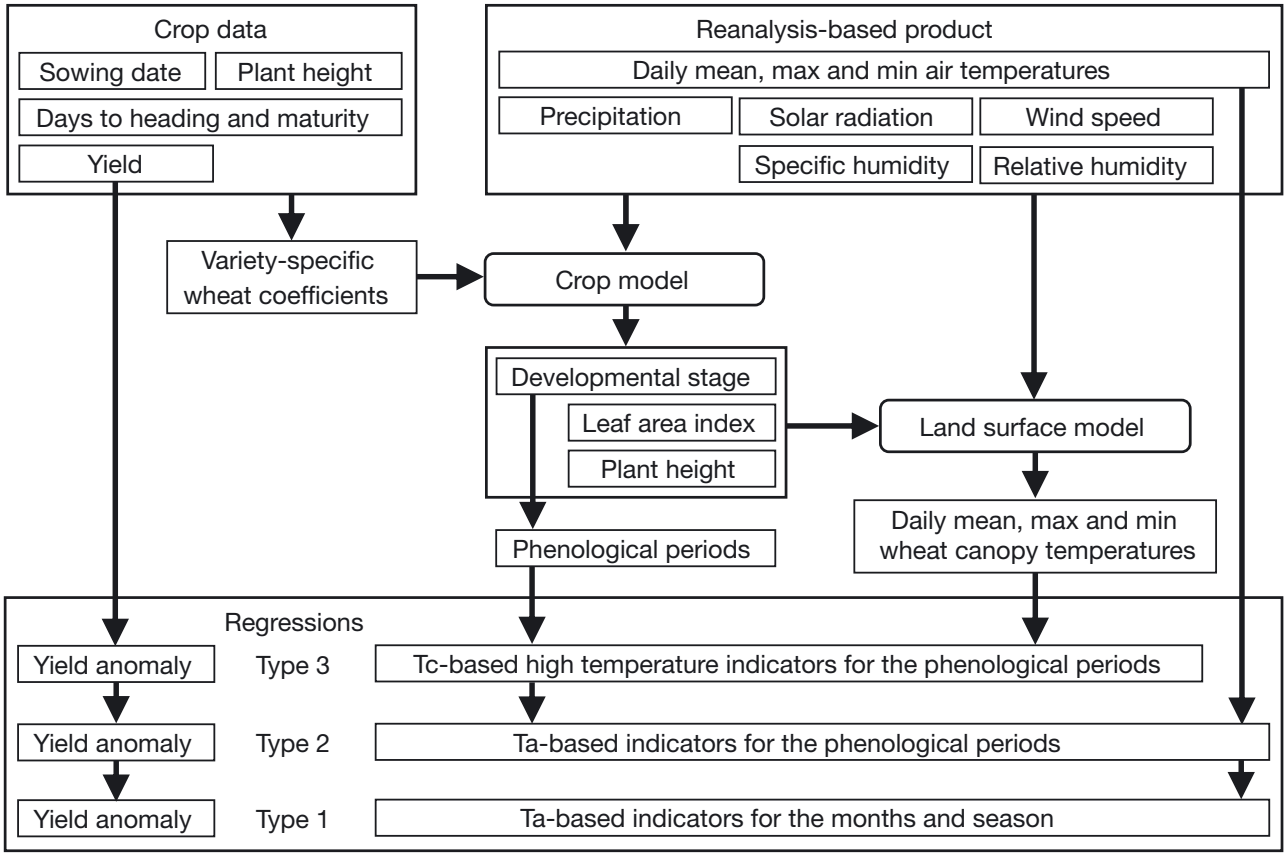

Fig. 1. Main data flow used in this study

The included regions were Dongola, Wad Medani, and New Halfa, which are located in the northern, central, and eastern parts of the country, respectively (Fig. 2). Data were lacking for 1984/85 in Wad Medani and for 1984/85, 2006/07, 2008/09, and 2009/10 in New Halfa. We found that the yields for 2016/17 and 2017/18 in Dongola and for 2004/05 in Wad Medani were not equal in value to the production volume divided by the harvested area (Fig. S1 in the Supplement at www.int-res.com/articles/suppl/c089p085_supp.pdf) and therefore were excluded from the analysis as unreliable records. We removed nonlinear trends that primarily represented the contributions of non-climatic factors from the yield time series using the smoothing spline in R version 4.0.4 ('smooth.spline' function with the number of knots to control the degree of smoothing ['nknots'] = 10) (R Core Team 2021). The trends in Dongola and New Halfa exhibited decadal fluctuations, while the trend in Wad Medani was characterized by a monotonic increase (Fig. 3). The amplitude of the yield anomaly was standardized, region by region.

We also collected field experimental data on sowing date and days to heading and maturity as well as plant height for 7 spring wheat varieties from the records of the Agricultural Research Corporation (ARC; Tahir et al. 2018) in Sudan (Table S1). The number of season–region–replication samples varied by variety

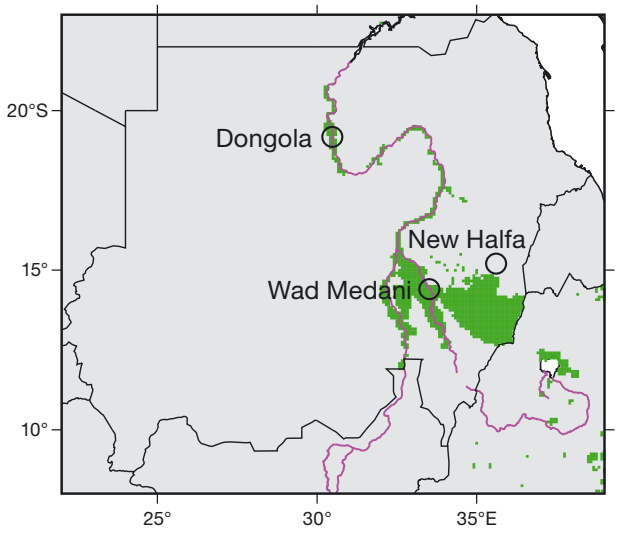

Fig. 2. Locations of the studied regions in Sudan. Purple lines indicate major river channels; green areas indicate irrigated wheat areas around the year 2010 (Yu et al. 2020)

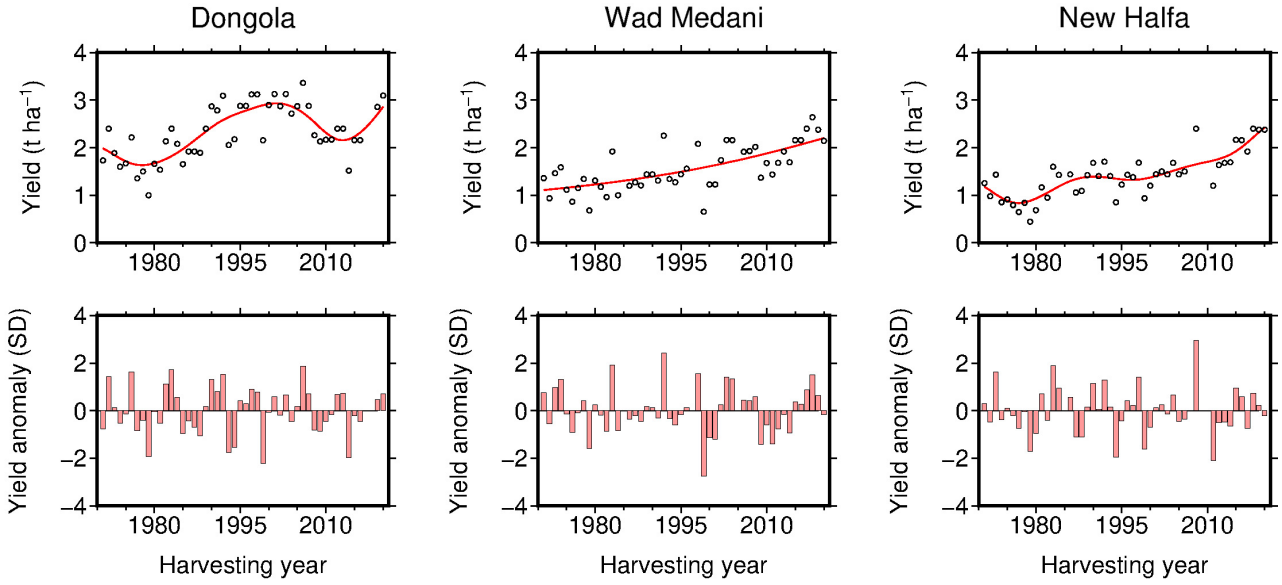

Fig. 3. Annual wheat yields, trends, and anomalies in the studied regions based on data from the 1970/71 to 2019/20 growing seasons. The red lines in the upper panels indicate the trend lines derived by fitting the smoothing spline

and ranged from 6 for Bohaine, Elneelain, Taghana, Wadi Elneel, and Zakia to 36 for Imam. These data were used to determine the variety-specific wheat coefficients input to the crop model (Fig. 1; see Section 2.3 for details).

2.2. Weather data

Three sources of weather data were used. First, the daily weather observations for the period 1970–2020 were collected from the Sudan Meteorological Authority (SMA) to compare with the reanalysis-based product described later. Another source was the micrometeorological observations from 1 February to 31 March 2019 collected at a wheat field (Imam cultivar) at the Gezira research station, Wad Medani. The micrometeorological data observed at a 10 minute resolution were aggregated into the daily data and compared with the simulated Tc. Lastly, daily data for the period 1971–2020 were acquired from a 0.5° resolution bias-corrected reanalysis product referred to as JRA-55–CDFDM–S14FD or JCS (Iizumi et al. 2021a). Since some weather variables required to run the crop model and the land surface model were lacking in the SMA observations, we used the reanalysis-based product for our analysis after validating it against the observations.

The weather variables for the reanalysis-based product were daily mean, maximum, and minimum 2 m air temperatures, relative humidity, specific humidity, solar radiation, and 10 m wind speed. This product was based on the Japanese 55-Year Reanalysis (JRA-55; Kobayashi et al. 2015, Harada et al. 2016) and bias-corrected using the cumulative distribution function-based downscaling method (CDFDM; Ishizaki et al. 2020) after spatial interpolation from 0.5625 to 0.5° resolution. The global retrospective meteorological forcing dataset S14FD (Iizumi et al. 2017b) for the period 1961–2000 was used as the reference for the bias correction. We selected a single 0.5° grid cell of the product that includes each station for the comparison. The relatively good agreement with the SMA observations confirmed that the product could be considered a reliable representation of the actual weather conditions for the studied season and regions (Fig. S2). However, the discrepancies between the 2 data sources were relatively larger for relative humidity, solar radiation, and wind speed than for the daily maximum and minimum air temperatures. The use of data values from only 1 station to compare with the mean value of a grid cell might be a reason for these differences. Nevertheless, we used the product for our analysis since it met the input requirements of the crop model and land surface model that were used to calculate Tc (Fig. 1).

2.3. Calculation of wheat canopy temperature

The Tc of wheat under irrigated conditions was obtained from the crop model and land surface model simulations. As these models were not coupled at the

moment of the analysis, we took a 2-step approach in which the developmental stage, leaf area index (LAI), and plant height simulated by the crop model were input to the land surface model (Fig. 1).

2.3.1. Crop model

We used the process-based global gridded crop yield growth model with assumptions on climate and socioeconomics (CYGMA; Iizumi et al. 2017a). The model has been used for variety-specific spring wheat simulations in Sudan (Iizumi et al. 2021a) as well as for global climate risk assessment (Jägermeyr et al. 2021). The model operates with a 0.5° resolution land grid cell and has a daily time step. Crop development, growth, and yields under rainfed and irrigated conditions were simulated separately, but only irrigated simulation outputs were used for the analysis.

Phenological development was modeled as a fraction of the accumulated growing degree days relative to the crop total thermal requirements and crop-specific base and upper temperatures. Leaf growth and senescence were calculated using the fraction of the growing season and prescribed shape of the LAI curve. Plant height was calculated using the prescribed shape of the plant height curve. Elevated CO_2 effects were considered for evapotranspiration rate, biomass, and yield but not for LAI and plant height. The actual evapotranspiration was calculated based on the soil water balance. Irrigation in the model increased the soil water content to 70% of the plant-extractable soil water capacity, which prevented the soil water content from being below that threshold level. This setting led to an irrigation frequency of about once per 10 d in the model, which matched the observed frequency in the central part of Sudan.

Five stress types, comprising nitrogen (N) deficit, heat, cold, water deficit, and water excess, were considered in the model. The most dominant stress type on a given day decreased the daily potential increase in the LAI and yield. The stress types, except for N deficit, were functions of daily weather, while the stress associated with N deficit was modeled as a function of the annual N application rate. Crop tolerance to these stresses increased as the knowledge stock increased. The knowledge stock is an economic indicator calculated as the sum of the national annual agricultural research and development expenditures since 1961 with a certain obsolescence rate, and represents the average technology level among farmers in a country. More modeling details and in-depth validation are available in Iizumi et al. (2021a).

The daily mean, maximum, and minimum 2 m air temperatures, precipitation, solar radiation, relative humidity, and 10 m wind speed obtained from the reanalysis-based product were input to the model (Fig. 1). The 10 m wind speed was corrected to that at the 2 m level using logarithmic profiles in the model. The plant-extractable water capacity of soils used in the model was based on Dunne & Willmott (1996). The historical annual changes in the N application rate and knowledge stock were fed into the model, as in Iizumi et al. (2021a). We also fed the variety-specific wheat coefficients determined based on the field experimental data described earlier (Fig. 1): the crop total thermal requirement from sowing to harvesting (GDDc), fraction of growing season at which flowering occurs ($fr_{GDD,ant}$), maximum plant height at an optimal condition (H_{max}), and maximum temperature for LAI growth and yield formation ($T_{u,heat}$) (Table S2). We assumed that the timing of flowering was close to heading due to the lack of flowering data. The plant height data for Bohaine, Elneelain, and Taghana were not available; therefore, the average of the remaining varieties was used. The $T_{u,heat}$ values were only available for Debeira and Imam (Iizumi et al. 2021a), and their average was used for the remaining varieties. The base and maximum temperatures for development were set to be the same across the varieties (18 and 32°C, respectively) due to the lack of information. The 49-season crop model simulations (1971/72 to 2019/20) were performed for the 35 combinations consisting of the 7 varieties and 5 sowing dates (15 November to 5 December, with a 5 d interval). The simulated developmental stage, LAI, and plant height for each variety and sowing date in the 0.5° grid cells corresponding to the locations of the studied regions were used as the inputs to the land surface model (Fig. 1).

2.3.2. Land surface model

We used the site-scale land surface model (Maruyama & Kuwagata 2010, Maruyama et al. 2017) to calculate wheat Tc. Although the model was originally developed for paddy rice, we applied it to irrigated wheat, given that wheat in Sudan is grown under fully irrigated conditions. The model solves 2 energy balance equations at an hourly time step: one is between the air and the crop canopy, and the other is between the air and the ground, with consideration of the water layer and crop growth. The model there-

fore assumes a saturated ground surface for the crop duration.

Daily mean, maximum, and minimum 2 m air temperatures, specific humidity, solar radiation, and wind speed obtained from the reanalysis-based product were used as the inputs (Fig. 1). The diurnal changes were estimated for each weather variable in the land surface model. The daily wheat phenological stage, LAI, and canopy height simulated by the crop model with irrigated conditions were also used as inputs. The maximum bulk stomatal conductance was set to change along with the wheat phenological stages, as was the case for rice in Maruyama et al. (2017). The wheat phenological stages simulated by the crop model ranged from 0 at sowing to approximately 0.6 at heading to 1 at maturity (Iizumi et al. 2021a), whereas the rice phenological stages originally used in the land surface model ranged from 0 at transplanting to 1 at heading and 2 at maturity (Maruyama & Kuwagata 2010). This occurred because the land surface model at the development phase presumes a rice growth model with a different model structure to that of the CYGMA model. To solve this inconsistency, we scaled the crop model-simulated phenological stage values to follow the definition used in the land surface model (Fig. S3). The inconsistent starting point in calculating crop growth (sowing in the crop model and transplanting in the land surface model) was left. However, the crop canopy has not yet matured at the beginning of the growth stage, and therefore the inconsistency does not much influence the difference between Ta and simulated Tc.

The 49-season simulations were performed for each variety–sowing date combination. The hourly outputs of the land surface model, including Tc, were converted into daily mean, maximum, and minimum values and then used to calculate the high-temperature indicators described in Section 2.4 (Fig. 1). The calculated daily mean differences between Tc and Ta in Wad Medani showed good agreement with the micrometeorological observations, with a correlation value of 0.582 and root mean squared error of 0.9°C (Fig. S4), although the samples were limited to 1 location and to 28 d in the latter part of one wheat season. The simulated daily mean Tc was slightly overestimated since the reanalysis-based daily mean 2 m Ta had a warmer bias. However, any biases in Tc do not affect the interpretations of the regression outcomes described later because biases in predictors do not change the signs of the regression coefficients.

2.4. High-temperature indicators

We explored 6 high-temperature indicators (Table 1): (1) average temperature, Tave; (2) average daily maximum temperature, Tmax; (3) average daily minimum temperature, Tmin; (4) THD; (5) THN; and (6) higher-than-optimal hourly temperature accumulation, DD. All of the indicators were calculated with either the reanalysis-based Ta or the simulated Tc. Tmax, Tmin, THD, and THN were adopted from Musa et al. (2021), while Tave and DD were newly added for the analysis. Tave is the simplest indicator. DD captures wheat exposure to high temperatures above the optimal level based on hourly temperatures obtained by fitting a sine curve to Tmax and Tmin. DD is conceptually the same as the extreme degree days (EDD) described by Lobell et al. (2012), with the temperature threshold value being the only difference: 18°C for this study according to Neitsch et al. (2005) and 34°C in Lobell et al. (2012). These indicators were calculated for 2 groups of time periods. One consisted of 5 calendar periods: the individual months from November to February and the entire season (NDJF). The other was composed of the 3 phenological periods simulated by the crop model (Fig. 1): the vegetative growth period (VGP), the reproductive growth period (RGP), and the whole

Table 1. High-temperature indicators explored in this study

Abbreviation	Unit	Description
Tave	°C	Average temperature for a certain period
Tmax	°C	Average daily maximum temperature for a certain period
Tmin	°C	Average daily minimum temperature for a certain period
THD	Fraction	Total number of hot days; the number of days with daily maximum temperature >35°C for a certain period[a]
THN	Fraction	Total number of hot nights; the number of days with daily minimum temperature >20°C for a certain period[a]
DD	°C hours	Higher-than-optimal hourly temperature accumulation for a certain period (optimal temperature = 18°C)[b]

[a]The threshold temperature value for THD and THN was set to be consistent with Musa et al. (2021)
[b]The optimal temperature value is based on Neitsch et al. (2005)

growth period (WGP). The Ta-based indicators calculated for the calendar months and season are shown in Fig. S5. The Ta- and Tc-based indicators calculated for the phenological periods are presented in Figs. S6 & S7, respectively. In the latter case, the indicators were calculated by variety and sowing date. Their average was used as the predictor in the regressions described in Section 2.5 (Fig. 1). The calculated indicators spanned the 49 seasons from 1971/72 to 2019/20.

2.5. Regressions

We conducted 3 types of regressions (Table 2): Type 1, which used Ta-based high-temperature indicators calculated for the calendar months and season and the linear specification; Type 2, which used the Ta-based indicators calculated for the phenological periods with consideration of the linear and nonlinear specifications; and Type 3, which were the same as Type 2 but used the Tc-based indicators (Fig. 1). In each case, the predictand was the yield anomaly described earlier (Fig. 3). The sample sizes were 47, 47, and 44 for Dongola, Wad Medani, and New Halfa, respectively, regardless of the regression type. Type 1 was a reproduction of Musa et al. (2021) using the updated data and modified yield detrending method and served as the baseline. The gains from using the phenological periods instead of the calendar months and season were assessed through comparisons of the Type 1 and Type 2 regressions, whereas the gains from using Tc rather than Ta were determined through comparisons of the Type 2 and Type 3 regressions.

The 2 model specifications, linear and nonlinear, were compared to evaluate whether the nonlinear specification consistently outperformed the linear specification in explaining the yield anomaly. The linear specification was computationally implemented in R using a general linear model ('lm' function), whereas the nonlinear specification was done using a generalized additive model (Hastie & Tibshirani 1990) ('gam' function). In the latter model, the predictand depends on a smooth function of a predictor derived by fitting a smoothing spline when a single predictor is considered. The smoothing parameter (*sp*) values were automatically determined in R to balance the model smoothness (the model complexity) and model prediction errors according to the generalized cross validation (GCV) criterion (Wood et al. 2016). The nonlinear specification becomes equivalent to the linear specification when larger *sp* values are adopted (Fig. S8). The superiority of the nonlinear specification relative to the linear specification was tested in R using ANOVA ('ANOVA' function). The null hypothesis used here was that there is no difference between the 2 specifications. If the null hypothesis was rejected at the 5% significance level, it indicated that the nonlinear specification is better than the linear specification. Furthermore, we visually checked the form of the estimated relationship between the predictors and predictand to avoid adopting nonlinear specifications with high-temperature–yield relationships contradictory to existing knowledge. The existing knowledge used here indicated a linear relationship with a negative slope or a convex upward quadratic relationship between high temperatures and yield reported in the literature (Lobell et al. 2012,

Table 2. Summary of regression analyses performed in this study. Ta (Tc): air (canopy)-based indicator; VGP (RGP, WGP): vegetative (reproductive, whole) growth period; other abbreviations as in Table 1

Type	Predictors		Specifications	Description
	Abbreviations[a]	Periods		
1	Tave.a, Tmax.a, Tmin.a, THD.a, THN.a, DD.a	Nov, Dec, Jan, Feb, whole season (NDJF)	Linear	Reproduction of Musa et al. (2021); serves as the baseline
2	Tave.a, Tmax.a, Tmin.a, THD.a, THN.a, DD.a	VGP, RGP, WGP	Linear, nonlinear	Comparisons between Type 1 and Type 2 regressions reveal the gains from using the phenological periods instead of months and season
3	Tave.c, Tmax.c, Tmin.c, THD.c, THN.c, DD.c	VGP, RGP, WGP	Linear, nonlinear	Comparisons between Type 2 and Type 3 regressions reveal the gains from using Tc instead of Ta

[a]The labels '.a' and '.c' refer to the Ta- and Tc-based high-temperature indicators, respectively

Asseng et al. 2015, 2017, Tack et al. 2015, Blanc 2020, Iizumi et al. 2021a).

Based on the regression results, we selected predictors for which the regression coefficients were significant at the 5% level and had a negative sign, indicating an adverse effect of high temperature on yield. We also calculated the adjusted coefficient of determination for the selected predictors as the measure of the variance of the yield anomaly explained by the predictor. The explained variance values for the selected predictors were presented in the form of a heatmap to extract a small number of predictors with moderate explanatory power that work well in multiple regions rather than a single region-specific indicator with the highest explanatory power. We allowed the time periods of the selected indicators to vary between the regions due to different wheat calendars.

3. RESULTS

3.1. Overview

This section provides an overview of the key results from the regressions, with a particular focus on the linear specification. As elaborated in Sections 3.3 and 3.4, the results from the linear specification proved to be more representative. The detailed results are described in the subsequent subsections.

In Dongola, comparisons of the Type 1 and Type 2 regressions revealed that using the timing and length of the phenological periods (VGP, in particular) substantially increased the explanatory power compared to using the indicators calculated for the calendar months and season (cf. left and right panels of Fig. 4). However, the gains from considering the phenological periods were not found for the RGP (Fig. 4). The comparisons of the Type 2 and Type 3 regressions showed that the gains from using Tc rather than Ta were minimal, if any, for Dongola. In Wad Medani, the results were diverse. The use of phenological periods and Tc increased the explanatory power when RGP was assessed (Fig. 4). However, the opposite was the case when WGP was evaluated; here, the explanatory power decreased with the consideration of phenology and Tc (Fig. 4). In New Halfa, the use of Tc for RGP consistently increased the explanatory power (cf. central and right panels of Fig. 4).

Tave, Tmax, Tmin, and DD for the key phenological periods (VGP in Dongola, WGP in Wad Medani, and RGP in New Halfa) were frequently selected to capture the adverse effects of high temperature on yield regardless of the region (Fig. 4). THD and THN were not powerful overall. Further comparisons of these selected indicators showed that the identification of VGP rather than considering Tc was the key to better explaining the yield anomaly for Dongola (Fig. 5), where the season average air temperature of

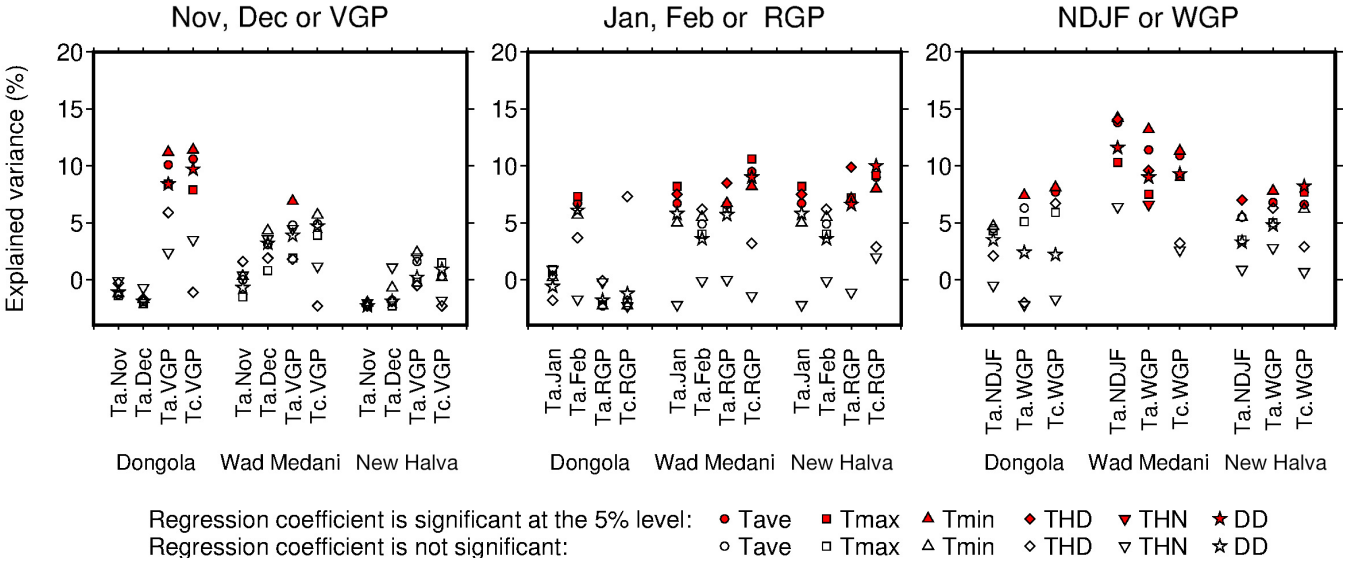

Fig. 4. Changes in explanatory power in response to using different wheat phenologies and canopy temperatures in the calculation of high-temperature indicators for 3 regions. Abbreviations as in Tables 1 & 2. Red-filled symbols denote that the regression coefficients of the indicators are significantly negative, while open symbols indicate that they are not. The regression coefficients were not successfully estimated for the Tc-based VGP THD in Dongola and Wad Medani due to the insufficient number of non-zero samples

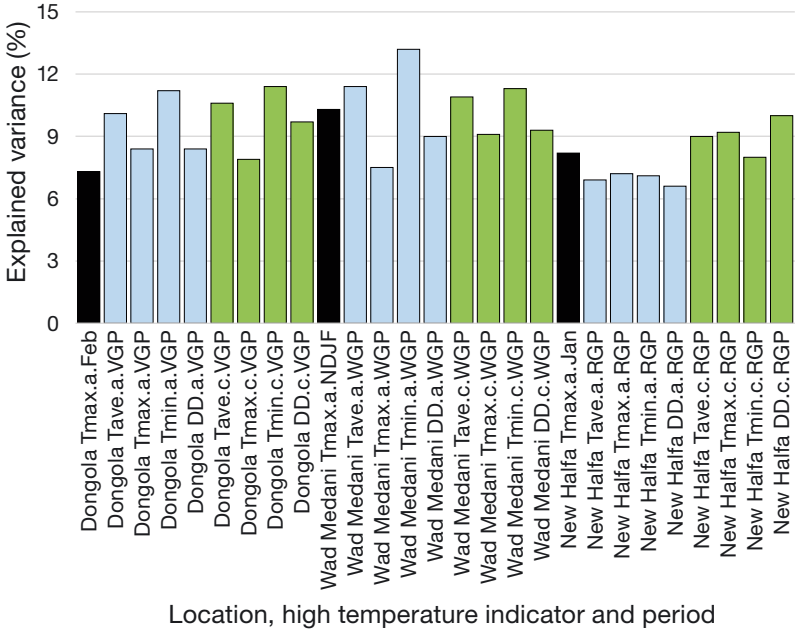

Fig. 5. Comparisons of the explanatory power between different high-temperature indicators selected in terms of multi-region applicability. Black, blue and green bars indicate Type 1, 2 and 3 regressions, respectively (see Table 2). Abbreviations as in Tables 1 & 2

Table 3. Heatmap showing the explanatory power when using the air temperature (Ta)-based high-temperature indicators calculated for the months and season, and the linear specification. Colored cells indicate significantly negative regression coefficients, while white cells denote that they are not significantly negative. More intense colors indicate larger explained variances. The explained variance values in percent are shown only for colored cells. Stippled cells indicate the indicators that commonly work relatively well throughout the regions (different time periods are accepted). Abbreviations as in Tables 1 & 2

Periods	Regions	High temperature indicators					
		Tave.a	Tmax.a	Tmin.a	THD.a	THN.a	DD.a
Nov.	Dongola						
	Wad Medani						
	New Halfa						
Dec.	Dongola						
	Wad Medani						
	New Halfa						
Jan.	Dongola						
	Wad Medani	7.2	7.9	6.8			
	New Halfa	6.7	8.2		7.5		
Feb.	Dongola	6.7	7.3				
	Wad Medani	7.3	6.9	6.7	8.3	1.1	6.5
	New Halfa						
Season (NDJF)	Dongola						
	Wad Medani	13.8	10.3	14.2	14.1		11.6
	New Halfa				7.0		

approximately 20°C was much lower than in the other 2 regions (Fig. S5). In New Halfa, where the season average air temperature (approximately 28°C) was the highest (Fig. S5), using the Tc-based indicators exhibited a clear advantage over using the Ta-based indicators. No clear benefit from using the Tc-based indicators was found for Wad Medani, where the season average air temperature was only slightly lower than that in New Halfa (about 26°C; Fig. S5). The identification of the phenological period (WGP) contributed to an increase in explanatory power only when Tave and Tmin were used; consideration of Tc did not increase explanatory power in the region.

3.2. Ta-based indicators for the months and season

The Type 1 regression results are summarized in Table 3. The high-temperature indicators (predictors) that were commonly selected throughout the regions were Tave and Tmax, although the selected time periods differed by region: February in Dongola, January and NDJF in Wad Medani, and January in New Halfa (stippled cells in Table 3). The explained variance was higher for Tmax than for Tave and spanned 6.7–7.3% in Dongola and 6.7–8.2% in New Halfa, with an opposite tendency for Wad Medani (10.3–13.8%). Although there were explained variance values greater than those noted above (e.g. 14.2% for NDJF Tmin in Wad Medani), we placed more emphasis on the indicators with multi-region applicability.

3.3. Ta-based indicators for the phenological periods

The Type 2 regression results are summarized in Table 4. The high-temperature indicator with a significantly negative regression coefficient that commonly appeared throughout the regions and specifications was Tmin. VGP and WGP Tmin were selected in Dongola, while only WGP Tmin was selected in Wad Medani and New Halfa. The explained variance values were nearly the same for the 2 specifications, with one exception: a substantial difference between the specifi-

Table 4. Same as in Table 3, but using the Ta-based high-temperature indicators calculated for the phenological periods and 2 specifications (linear and nonlinear)

Periods	Regions	Specifications	High temperature indicators					
			Tave.a	Tmax.a	Tmin.a	THD.a	THN.a	DD.a
VGP	Dongola	Linear	10.1	8.4	11.2			8.4
		Nonlinear	11.4		11.6		19.0	13.5
	Wad Medani	Linear			6.9			
		Nonlinear						
	New Halfa	Linear						
		Nonlinear						
RGP	Dongola	Linear						
		Nonlinear						
	Wad Medani	Linear	6.6		6.7	8.5		
		Nonlinear				8.6		20.6
	New Halfa	Linear	6.9	7.2	7.1	9.9		6.6
		Nonlinear				9.7		
WGP	Dongola	Linear			7.4			
		Nonlinear	16.9	15.1	16.3			18.8
	Wad Medani	Linear	11.4	7.5	13.2	9.6	6.6	9.0
		Nonlinear	11.3		13.3	9.5		8.9
	New Halfa	Linear	6.8		7.8			
		Nonlinear			7.8			

cations was found for WGP Tmin in Dongola (7.4% for the linear specification and 16.3% for the nonlinear specification). However, the ANOVA results showed that the nonlinear specification rarely outperformed the linear specification (Table 5). WGP Tmin in Dongola was one of the few examples. Nevertheless, visual assessment suggests that the estimated relationship between WGP Tmin and the yield anomaly in Dongola, where the yield decreased with an increase in WGP Tmin and became less sensitive to an increase in WGP Tmin once WGP Tmin exceeded 12°C (Fig. S9), was somewhat contradictory to existing knowledge. Therefore, adopting the nonlinear specification for WGP Tmin in Dongola was not thought to be justified.

Table 5. Heatmap showing the superiority of the nonlinear specification relative to the linear specification based on the ANOVA results for the air temperature (Ta)-based high-temperature indicators calculated for the phenological periods. Light green cells indicate the cases in which the nonlinear specification was superior

Periods	Regions	High temperature indicators					
		Tave.a	Tmax.a	Tmin.a	THD.a	THN.a	DD.a
VGP	Dongola						
	Wad Medani						
	New Halfa						
RGP	Dongola						
	Wad Medani						
	New Halfa						
WGP	Dongola						
	Wad Medani						
	New Halfa						

3.4. Tc-based indicators for the phenological periods

In the Type 3 regression, many more indicators were commonly selected throughout the regions and specifications than in the other regression types described earlier. The selected 11 region-indicator cases included VGP Tave, Tmax, and DD in Dongola; RGP Tave and DD and WGP Tave and Tmax in Wad Medani; and RGP Tave, Tmax, and DD and WGP Tave in New Halfa (Table 6). Although the explained variance values were always greater for the nonlinear specification than for the linear specification (Table 6), the statistical tests showed that the significant superiority of the nonlinear specification was detected in only 3 of the 11 region-indicator cases: VGP DD and WGP Tave in Dongola and WGP Tave in New Halfa (Table 7). However, visual checks (Figs. S10–S12) suggested a convex downward quadratic relationship for VGP DD and WGP Tave in Dongola (Fig. S10), and a cubic relationship was evident for WGP Tave in New Halfa (Fig. S12), leading to a rejection of the non-

Table 6. Same as in Table 4, but for the canopy temperature (Tc)-based high-temperature indicators

Periods	Regions	Specifications	High temperature indicators					
			Tave.c	Tmax.c	Tmin.c	THD.c	THN.c	DD.c
VGP	Dongola	Linear	10.6	7.9	11.4			9.7
		Nonlinear	14.5	14.4	14.3			24.4
	Wad Medani	Linear						
		Nonlinear						
	New Halfa	Linear						
		Nonlinear						
RGP	Dongola	Linear						
		Nonlinear						
	Wad Medani	Linear	9.5	10.6	8.2			9.0
		Nonlinear	11.6					11.9
	New Halfa	Linear	9.0	9.2	8.0			10.0
		Nonlinear	9.7	9.7				12.3
WGP	Dongola	Linear	7.7		8.1			
		Nonlinear	20.1	18.6	20.1			18.5
	Wad Medani	Linear	10.9	9.1	11.3			9.3
		Nonlinear	11.0	8.9				9.3
	New Halfa	Linear	6.6	7.7				8.2
		Nonlinear	20.1		18.8			

linear specification due to the inconsistency with existing knowledge. The explanatory power of the linear specification for the selected indicators (11 cases) spanned 7.9–10.6% in Dongola, 9.0–10.9% in Wad Medani, and 6.6–10.0% in New Halfa (Table 6).

4. DISCUSSION

There were 2 major differences between our reproduction (the Type 1 regressions) and the results of Musa et al. (2021). First, Musa et al. (2021) found significant negative correlations for November in Dongola and New Halfa. This is difficult to interpret, as November corresponds to preseason or sowing, and high temperatures during that month have no direct influence on yield. Second, Musa et al. (2021) found few significantly negative correlations for February. However, grain filling in Sudan generally occurs in February (FAO 2021), and high temperatures during that month adversely affect yields. The results reported by Musa et al. (2021), which contradict local knowledge, are explained in our reproduction. Significant adverse effects from high air temperatures on yield were detected for February in Dongola, January to February and NDJF in Wad Medani, and mostly January in New Halfa in our reproduction (Table 3). Replacing the linear trends used by Musa et al. (2021) for detrending yield time series with nonlinear trends is likely the reason for the reconciled results. Excluding unreliable yield records from the analysis and adding new yield samples also contributed to the discrepancy between Musa et al.'s (2021) results and our own. On the other hand, the use of different sources of air temperature data between studies was evidently not the reason for this discrepancy given the close agreement between the observations and the reanalysis-based product ('Tx' and 'Tn' in Fig. S2).

Table 7. Same as Table 5 but for the canopy temperature (Tc)-based high-temperature indicators

Periods	Regions	High temperature indicators					
		Tave.c	Tmax.c	Tmin.c	THD.c	THN.c	DD.c
VGP	Dongola						
	Wad Medani						
	New Halfa						
RGP	Dongola						
	Wad Medani						
	New Halfa						
WGP	Dongola						
	Wad Medani						
	New Halfa						

Adding processes into the indicator calculation from the Type 1 to Type 3 regressions contributed to the identification of clearer high-temperature effects on yield and their key periods. The Tc-based Tave, Tmax, and DD demonstrated relatively ro-

bust multi-region applicability, although they did not necessarily provide the greatest explanatory power between the regression types. The frequent selections of the Tc-based Tave and Tmax and, to a lesser extent, Tmin suggest that all aspects of the season canopy temperature contribute to explaining yield reductions. This finding leads to the hypothesis that more complete information on wheat exposure to high canopy temperatures during a day, and its accumulation for a key phenological period, will increase explanatory power as compared to information on specific aspects of the season canopy temperature alone (Tave, Tmax, and Tmin). However, DD did not always outperform the other indicators (Table 6). DD is an illustrative specification designed to contain more complete seasonal canopy temperature information and does not preclude the possibility of other specifications, which is a subject worth exploring in future research.

The explained variance values for the Tc-based indicators are small in absolute terms. Using more accurate Tc data may improve the explanatory power. The limited micrometeorological data used in the study (Fig. S4) prevented a more complete assessment of the crop model and land surface model simulations, and future research will be necessary in order to produce more conclusive results in this regard. In addition, information on the adoption rates and sowing dates of individual varieties, as well as any historical changes in their values, if available, will help to simulate Tc more precisely, since there is accumulated evidence showing changes in crop phenology during the last decades due to crop variety changes and climate warming (Asseng et al. 2017, Rezaei et al. 2018). Lastly, nonclimatic factors, such as year-to-year currency exchange rate fluctuations (Elbushra et al. 2010, Elsheikh et al. 2012) and changes in irrigation performance over time (Salih et al. 1994, Al Zayed et al. 2015), might also cause errors in efforts to explain yield anomalies using climate conditions alone. Al Zayed et al. (2015) reported that poor irrigation performance has occurred in the central region of Sudan since the 1993/1994 season. Although the average frequency of irrigation applications in the crop model was calibrated to match the observed frequency (roughly once per 10 d), the reported decreasing trend in irrigation performance was not considered in the analysis. Given the possibility that irrigation efficiency could decline when the production area expands and, hence, affect yield, irrigation efficiency is a matter worth studying in the future. Currently, however, relevant data are not available.

Our results indicate that in the relatively cooler region (Dongola), high-temperature effects on the processes during the VGP (a shortened grain-filling period, for instance) are likely a dominant factor in yield reduction, while high-temperature effects on the processes during the RGP are not. Rapid growth under warmer conditions, together with the associated reduction in the grain-filling period, are a well-documented process that reduces yield even in the absence of heat stress (e.g. Tao et al. 2006, Rezaei et al. 2015b). In the relatively hot regions (New Halfa, in particular), it is suggested that the high-temperature effects on the processes during the RGP, such as a decrease in photosynthetic rate, seed number, grain-filling period, and rate, as well as an increase in maintenance respiration and pollen sterility, may be a more dominant influence on yield reduction than the high-temperature effects on the processes during the VGP. The season average air temperature conditions during flowering and grain filling in Dongola were likely close to the optimal level (21°C; Sánchez et al. 2014), whereas those in New Halfa were hotter than that level (Fig. S7). As a result, the influence of high-temperature effects during the RGP are more clearly highlighted in New Halfa than in Dongola. In Wad Medani, high-temperature effects on the processes during both the RGP and WGP would likely play a role and make it more difficult to explain the yield anomaly with a single high-temperature indicator.

Tc-based high-temperature indicators could play a role in agrometeorological services aiming to strengthen the capability of societies to seamlessly manage climate risk in crop production systems, from high-temperature extremes to long-term changes in mean temperature. Daily weather and crop calendars are the main inputs for calculating canopy temperature using models such as those employed in this study. Weather data are available for wheat-producing regions across the world from various reanalysis-based data products (Toreti et al. 2019), including the one used in this study. Global wheat calendars have become increasingly available and have improved substantially during the past decade (Kim et al. 2021). Improvements in weather and crop calendar data products, as well as recent increases in computational capacity for model simulations, make crop-specific Tc-based indicators available for national- to global-scale applications. This can supplement not only national agrometeorological services but also global agricultural monitoring and forecasting services (Fritz et al. 2019, Iizumi et al. 2021b). Information on wheat varietal characteristics important to accurately calculate canopy temperature is still lacking, but available field experimental data can be used, as in this study.

5. CONCLUSIONS

Agrometeorological services, including crop monitoring and forecasting, constitute a sector-specific climate service. Given the increasing need for adaptation to climate change in agriculture, we propose high-temperature indicators to capture yield reductions associated with heat stress, using irrigated wheat in Sudan as a case study. The benefits of using canopy temperature rather than air temperature are especially clear in regions where high-temperature effects on processes during the reproductive growth period are the principal determinant of yield reductions. Canopy temperature-based high-temperature indicators (especially the average canopy temperature) calculated for region-specific key phenological periods show relatively robust multi-region applicability and can therefore be viewed as promising candidate indicators. In most cases, no significant difference in explanatory power was found between the linear and nonlinear specifications. However, with yield data at the regional scale, as was the case for the yield data in this study, the nonlinear specification often produced uninterpretable temperature–yield relationships compared to those at the field scale reported in the literature. Thus, caution is necessary if the data are to be used for national- or global-scale applications. Given the recent increases in data availability and computing power, we encourage the incorporation of canopy temperature-based high-temperature indicators into agrometeorological services.

Acknowledgments. We thank Prof. I. E. A. Ali-Babiker for his support in data collection in the early stages of this study. The crop model simulations were conducted at the High-Performance Cluster Computing System at the Agriculture, Forestry and Fisheries Research Information Technology Center, the Ministry of Agriculture, Forestry and Fisheries. This study was funded by the Joint Research Program of Arid Land Research Center, Tottori University (No. 02F2001 to T.I.) and JST SATREPS (JPMJSA1805 to H.T.). T.I. was partly supported by Grants-in-Aid for Scientific Research (22H00577 and 20K06267) from the Japan Society for the Promotion of Science; and the Environment Research and Technology Development Fund (JPMEERF20202002) of the Environmental Restoration and Conservation Agency Provided by the Ministry of Environment of Japan.

LITERATURE CITED

Amani I, Fischer RA, Reynolds MP (1996) Canopy temperature depression association with yield of irrigated spring wheat cultivars in a hot climate. J Agron Crop Sci 176:119–129

Asseng S, Ewert F, Martre P, Rötter RP and others (2015) Rising temperatures reduce global wheat production. Nat Clim Change 5:143–147

Asseng S, Cammarano D, Basso B, Chung U and others (2017) Hot spots of wheat yield decline with rising temperatures. Glob Change Biol 23:2464–2472

Asseng S, Martre P, Maiorano A, Rötter RP and others (2019) Climate change impact and adaptation for wheat protein. Glob Change Biol 25:155–173

Barlow KM, Christy BP, O'Leary GJ, Riffkin PA, Nuttall JG (2015) Simulating the impact of extreme heat and frost events on wheat crop production: a review. Field Crops Res 171:109–119

Blanc É (2020) Statistical emulators of irrigated crop yields and irrigation water requirements. Agric Meteorol 284:107828

Brisson N, Mary B, Ripoche D, Jeuffroy MH and others (1998) STICS: a generic model for the simulation of crops and their water and nitrogen balances. I. Theory and parameterization applied to wheat and corn. Agronomy 18:311–346

Dunne KA, Willmott CJ (1996) Global distribution of plant-extractable water capacity of soil. Int J Climatol 16: 841–859

Elbushra AA, Elsheikh OE, Salih AAA (2010) Impact of exchange rate reforms on Sudan's economy: applied general equilibrium analysis. Afr J Agric Res 5:442–448

Elsheikh OE, Elbushra AA, Salih AAA (2012) Impacts of changes in exchange rate and international prices on agriculture and economy of the Sudan: computable general equilibrium analysis. Sustain Agric Res 1:201–210

FAO (Food and Agriculture Organization of the United Nations) (2021) GIEWS — Global Information and Early Warning System. Country Briefs. Sudan. www.fao.org/giews/countrybrief/country.jsp?code=SDN (accessed 7 September 2021)

Fritz S, See L, Bayas JCL, Waldner F and others (2019) A comparison of global agricultural monitoring systems and current gaps. Agric Syst 168:258–272

Fukuoka M, Yoshimoto M, Hasegawa T (2012) Varietal range in transpiration conductance of flowering rice panicle and its impact on panicle temperature. Plant Prod Sci 15:258–264

Harada Y, Kamahori H, Kobayashi C, Endo H and others (2016) The JRA-55 Reanalysis: representation of atmospheric circulation and climate variability. J Meteorol Soc Jpn 94:269–302

Hastie T, Tibshirani R (1990) Generalized additive models. Chapman & Hall, London

Iizumi T, Furuya J, Shen Z, Kim W and others (2017a) Responses of crop yield growth to global temperature and socioeconomic changes. Sci Rep 7:7800

Iizumi T, Takikawa H, Hirabayashi Y, Hanasaki N, Nishimori M (2017b) Contributions of different bias-correction methods and reference meteorological forcing data sets to uncertainty in projected temperature and precipitation extremes. J Geophys Res Atmos 122:7800–7819

Iizumi T, Ali-Babiker IEA, Tsubo M, Tahir ISA and others (2021a) Rising temperatures and increasing demand challenge wheat supply in Sudan. Nat Food 2:19–27

Iizumi T, Shin Y, Choi J, van der Velde M, Nisini L, Kim W, Kim KH (2021b) Evaluating the 2019 NARO-APCC Joint Crop Forecasting Service yield forecasts for Northern Hemisphere countries. Weather Forecast 36:879–891

Ishizaki NN, Nishimori M, Iizumi T, Shiogama H, Hanasaki N, Takahashi K (2020) Evaluation of two bias-correction methods for gridded climate scenarios over Japan. Sci Online Lett Atmos 16:80–85

Jägermeyr J, Müller C, Ruane AC, Elliott J and others (2021) Climate impacts on global agriculture emerge earlier in

new generation of climate and crop models. Nat Food 2: 873–885
Jamieson PD, Brooking IR, Porter JR, Wilson DR (1995) Prediction of leaf appearance in wheat: a question of temperature. Field Crops Res 41:35–44
Kim KH, Doi Y, Ramankutty N, Iizumi T (2021) A review of global gridded cropping system data products. Environ Res Lett 16:093005
Kobayashi S, Ota Y, Harada Y, Ebita A and others (2015) The JRA-55 Reanalysis: general specifications and basic characteristics. J Meteorol Soc Jpn 93:5–48
Lobell DB, Sibley A, Ortiz-Monasterio JI (2012) Extreme heat effects on wheat senescence in India. Nat Clim Change 2:186–189
Martre P, Reynolds MP, Asseng S, Ewert F and others (2017) The International Heat Stress Genotype Experiment for modeling wheat response to heat: field experiments and AgMIP-Wheat multi-model simulations. Open Data J Agric Res 3:23–28
Maruyama A, Kuwagata T (2010) Coupling land surface and crop growth models to estimate the effects of changes in the growing season on energy balance and water use of rice paddies. Agric For Meteorol 150:919–930
Maruyama A, Nemoto M, Hamasaki T, Ishida S, Kuwagata T (2017) A water temperature simulation model for rice paddies with variable water depths. Water Resour Res 53:10065–10084
Mbow C, Rosenzweig C, Barioni LG, Benton TG and others (2019) Food security. In: Shukla PR, Skea J, Calvo Buendia E, Masson-Delmotte V and others (eds) Climate change and land: an IPCC special report on climate change, desertification, land degradation, sustainable land management, food security, and greenhouse gas fluxes in terrestrial ecosystems. IPCC, Geneva, p 437–550
Musa AII, Tsubo M, Ali-Babiker IEA, Iizumi T and others (2021) Relationship of irrigated wheat yield with temperature in hot environments of Sudan. Theor Appl Climatol 145:1113–1125
Negassa A, Shiferaw B, Koo J, Sonder K and others (2013) The potential for wheat production in Africa: analysis of biophysical suitability and economic profitability. CIMMYT, Mexico, DF
Neitsch SL, Arnold JG, Kiniry JR, Williams JR (2005) Soil and water assessment tool theoretical documentation (Version 2005). USDA, Temple, TX
R Core Team (2021) R: a language and environment for statistical computing. R Foundation for Statistical Computing, Vienna
Rezaei EE, Webber H, Gaiser T, Naab J, Ewert F (2015a) Heat stress in cereals: mechanisms and modelling. Eur J Agron 64:98–113
Rezaei EE, Siebert S, Ewert F (2015b) Intensity of heat stress in winter wheat — phenology compensates for the adverse effect of global warming. Environ Res Lett 10:024012
Rezaei EE, Siebert S, Hüging H, Ewert F (2018) Climate change effect on wheat phenology depends on cultivar change. Sci Rep 8:4891
Salih AEM, Abdalla OA, Sidahmed M, Faki H, Ismail MA (1994) Wheat production in the Gezira Scheme. In: Saunders DA, Hettel GP (eds) Wheat in heat-stressed environments: irrigated, dry areas and rice–wheat farming systems. CIMMYT, Mexico, DF, p 75–77
Sánchez B, Rasmussen A, Porter JR (2014) Temperatures and the growth and development of maize and rice: a review. Glob Change Biol 20:408–417
Shew AM, Tack JB, Nalley LL, Chaminuka P (2020) Yield reduction under climate warming varies among wheat cultivars in South Africa. Nat Commun 11:4408
Siebert S, Ewert F, Rezaei EE, Kage H, Graß R (2014) Impact of heat stress on crop yield — on the importance of considering canopy temperature. Environ Res Lett 9: 044012
Tack J, Barkley A, Nalley LL (2015) Effect of warming temperatures on US wheat yields. Proc Natl Acad Sci USA 112:6931–6936
Tahir ISA, Mustafa HM, Saad ASI, Elbashier EME and others (2018) Grain yield and stability of elite stem and leaf rusts resistant bread wheat genotypes under the hot environments of Sudan: a proposal for the release of three bread wheat varieties. National Variety Release Committee Meeting, Khartoum
Tao F, Yokozawa M, Xu Y, Hayashi Y, Zhang Z (2006) Climate changes and trends in phenology and yields of field crops in China, 1981–2000. Agric For Meteorol 138:82–92
Toreti A, Maiorano A, De Sanctis G, Webber H and others (2019) Using reanalysis in crop monitoring and forecasting systems. Agric Syst 168:144–153
van Oort PAJ, Saito K, Zwart SJ, Shrestha S (2014) A simple model for simulating heat induced sterility in rice as a function of flowering time and transpirational cooling. Field Crops Res 156:303–312
Webber H, Ewert F, Kimball BA, Siebert S and others (2016) Simulating canopy temperature for modelling heat stress in cereals. Environ Model Softw 77:143–155
Webber H, Martre P, Asseng S, Kimball B and others (2017) Canopy temperature for simulation of heat stress in irrigated wheat in a semi-arid environment: a multi-model comparison. Field Crops Res 202:21–35
WMO (2021) Expert Team on Climate Information for Decision-Making. https://community.wmo.int/governance/commission-membership/commission-weather-climate-water-and-related-environmental-service-applications-sercom/commission-services-officers/sercom-management-group/standing-committee-climate-services/expert-team-climate-information-decision (accessed 4 September 2021)
Wood SN, Pya N, Säfken B (2016) Smoothing parameter and model selection for general smooth models. J Am Stat Assoc 111:1548–1563
Yoshimoto M, Fukuoka M, Hasegawa T, Utsumi M, Ishigooka Y, Kuwagata T (2011) Integrated micrometeorology model for panicle and canopy temperature (IM^2PACT) for rice heat stress studies under climate change. J Agric Meteorol 67:233–247
Yoshimoto M, Fukuoka M, Hasegawa T, Matsui T and others (2012) MINCERnet: a global research alliance to support the fight against heat stress in rice. J Agric Meteorol 68:149–157
Yu Q, You L, Wood-Sichra U, Ru Y and others (2020) A cultivated planet in 2010. 2. The global gridded agricultural-production maps. Earth Syst Sci Data 12:3545–3572
Zayed ISA, Elagib NA, Ribbe L, Heinrich J (2015) Spatio-temporal performance of large-scale Gezira Irrigation Scheme, Sudan. Agric Syst 133:131–142

Editorial responsibility: Davide Cammarano, West Lafayette, Indiana, USA
Reviewed by: 3 anonymous referees

Submitted: June 10, 2022
Accepted: January 3, 2023
Proofs received from author(s): January 30, 2023